SE9400030

TRITA-ALP-1993-02
Report
ISSN 1103-6613
ISRN KTH/ALP/R--93/2--SE

KTH

The Double Probe Electric Field Experiment on Freja: Description and First Results

G.T. Marklund et al.

TRITA - ALP - 93 - 02

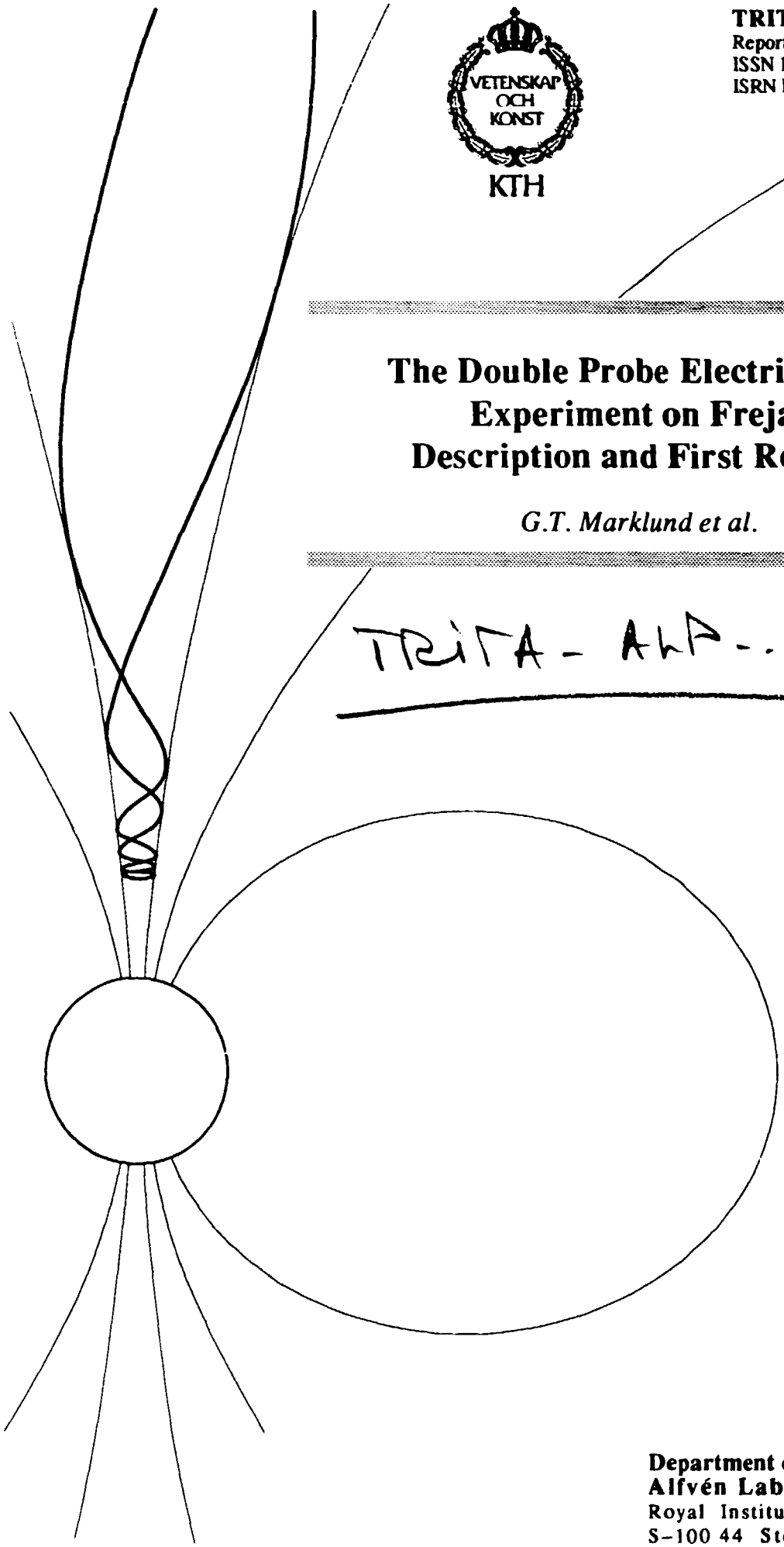

Department of Plasma Physics
Alfvén Laboratory
Royal Institute of Technology
S-100 44 Stockholm, Sweden

THE DOUBLE PROBE ELECTRIC FIELD EXPERIMENT ON FREJA: DESCRIPTION AND FIRST RESULTS

G. T. Marklund, L. G. Blomberg, P.-A. Lindqvist, and C.-G. Fälthammar

Department of Plasma Physics, Alfvén Laboratory,
Royal Institute of Technology, Stockholm, Sweden

G. Haerendel

Max-Planck-Institut für Extraterrestrische Physik,
Garching, Germany

F. S. Mozer

Space Sciences Laboratory, University of California,
Berkeley, CA, USA

A. Pedersen

Space Science Department, ESTEC,
Noordwijk, The Netherlands

P. Tanskanen

Department of Physics, University of Oulu,
Oulu, Finland

October 1993

Abstract. A description is given of the Freja double-probe electric field instrument. Its capability to perform high-resolution measurements of the aurora and its fine-structure as well as collect information on sub-auroral and low-latitude phenomena is illustrated by selected results from the first six months of operation. The instrument is highly flexible and possible to operate in a number of different modes. It is also equipped with a 4-Megabyte burst memory for high data sampling rate and temporary storage of data. It has been fully operational since October 1992, and delivers data from ≈22 hours/day including about 5–6 auroral crossings/day of the northern and southern auroral ionosphere. New and important information on the auroral fine structure and electrodynamics is obtained by means of burst resolution data (6144 samples/s) and normal resolution data (768 samples/s). Common burst data collection triggered by the electric field event detector has turned out to be very useful for the selection of scientifically interesting events. This is illustrated by high-resolution data of a pair of extremely intense and narrow electric field structures (1 V/m) which are associated with a total absence of precipitating particles, depletions of the thermal plasma and with an intense wave activity. The low inclination of the Freja orbit provides a new perspective for studying large-scale phenomena associated with east-west gradients as is exemplified by electric field data from a satellite crossing over north-south oriented auroral structures presumably resulting from rotational distortions of east-west aligned auroral arcs. The different plasma regimes encountered by Freja are continuously monitored by means of current sweeps applied to the probes and by the satellite potential. In addition, overview data (8 samples/s) are collected from full orbits and stored in the on-board memory and have proved to be extremely valuable, providing new information on global electric field phenomena at subauroral and lower latitudes, such as the intense poleward electric fields and Pc–1 observations that have been made near the plasmapause during substorm activity.

1. Introduction

The Freja mission is aimed at studying, in great detail, the physics of the fine-structured and dynamic plasma of the upper auroral ionosphere and the innermost magnetosphere. The altitude range that is explored by Freja (600 km – 1700 km) forms an interesting transition region between the ionosphere, where the auroral displays and associated energy dissipation processes take place, and the auroral acceleration regions where the auroral particles become energized. High-altitude rocket observations of intense electric field fluctuations, similar to what has been observed by the S3-3, DE 1 and Viking satellites at higher altitudes within and above the auroral acceleration regions, suggest that these may occasionally extend down to the upper ionosphere below 1000 km. Further, ion conical distributions and upward ion beams, frequently observed by Viking and S3-3, are believed to predominantly originate at Freja altitudes.

The Freja electric field experiment has a normal sampling rate of 768 samples/s, which is 15 times higher than that of Viking. For shorter time periods ($\approx$1 min) a sampling rate of 6144 samples/s is used to examine the fine-scale structures in even more detail. The high telemetry rate and thus temporal resolution of the Freja instrumentation as compared to earlier satellites, makes it ideally suited for studying the many complicated phenomena of the ionosphere-magnetosphere transition region.

2. Scientific Objectives

2.1 Auroral particle acceleration

The objective is to further explore (and estimate the relative roles of) various suggested mechanisms to maintain quasi-dc parallel electric fields (such as double layers and weak double layers, anomalous resistivity and magnetic mirror effects).

The Viking observations in the auroral acceleration region have demonstrated a considerable degree of spatial and temporal structure associated with, for example, electrostatic shocks, weak double layers and low-frequency fluctuations [e.g., *Boström et al.*, 1988; *Marklund*, 1993; *Mälkki et al.*, 1993; cf. also *Temerin et al.*, 1982]. The observations suggest a modified potential well structure with fluctuating potential contours and a parallel potential drop extended over a large region parallel to **B** (1000 km) that may occasionally extend down to Freja altitudes.

The intense (500 mV/m or more) irregular electric fields at various scale sizes reaching down to the resolution of the measurement, typically occur in conjunction with upgoing ion beams or conics, with low-density plasma fluctuations and with intense field-aligned currents. The Viking results [e.g., *Lindqvist and Marklund*, 1990] as well as the Dynamics Explorer 1 and 2 intercomparisons [e.g., *Weimer et al.*, 1985] show that the electric fields at smaller wavelengths become much more intense at higher altitudes whereas the large-scale features remain roughly unchanged with altitude. This difference between the high-altitude and low-altitude electric fields suggests that parallel electric fields must exist somewhere in between. There are several mechanisms that might support parallel electric fields such as double layers, anomalous resistivity, magnetic mirror effects, etc., and it is important to further examine and estimate the relative roles of these.

Low-frequency electric field fluctuations (< 1 Hz) have been found to be a common feature on auroral flux tubes (at practically all local times and for all activity levels). The fluctuations play an important role in the acceleration of auroral particles [e.g., *Hultqvist*, 1988; *Hultqvist et al.*, 1991; *André and Eliasson*, 1992]. In this frequency range the electric field appears as static for the electrons but not for the ions, giving rise to a selective acceleration. The fluctuations are likely to contribute to the thermal energy of the closely associated escaping ionospheric ions [e.g., *Lundin et al.*, 1990].

The much improved resolution of the Freja measurements as compared to earlier spacecraft, the burst memory capability, plus the possibility of simultaneous vector electric field (4 probes) and interferometric density measurements (2 probes) provide a most powerful means to investigate the lower parts of the auroral acceleration region, in great detail.

2.2 Auroral electrodynamics

The objective is to study the formation, energy transfer and current closure mechanisms of different auroral structures or arc systems (such as the Westward Travelling Surge (WTS), multiple arcs, the auroral horn, etc.) and to obtain a better understanding of the relationships between currents, electric fields, particles, and optical emissions for these.

Whereas the Viking mission was ideal for studies of global or large-scale auroral distributions and associated electrodynamics [e.g., *Marklund and Blomberg*, 1991; *Blomberg and Marklund*, 1993], the Freja mission is ideal for studies of the smaller structures from scale sizes of auroral rays to those comparable to the width of the auroral oval. Due to the relatively low inclination of the orbit Freja is best suited for studies of nightside auroral features such as the discrete evening aurora, multiple arcs, the WTS etc. The Freja orbit often crosses the auroral oval at a relatively small angle, which implies good opportunities to explore regions or phenomena associated with large east-west gradients, such as the Harang discontinuity. With a similar resolution to rockets but with much improved continuous coverage, Freja may contribute significantly to our understanding of current closure mechanisms, energy transfer and formation associated with such night-side auroral structures.

Detailed relationships between boundaries, as defined by different instrumental parameters (such as convection reversals, field-aligned current regions, particle and optical boundaries) need to be further explored and are ideally suited for Freja in the context of both the large-scale auroral oval and small-scale discrete arcs.

2.3 Sub-auroral and equatorial phenomena

The relatively low inclination orbit of Freja makes it well suited for studies of sub-auroral phenomena since it spends extended periods of time in this region, rather than cutting across quickly like polar orbiting satellites. Of particular interest are sub-auroral electric fields and the penetration of the auroral electric fields to lower latitudes. This includes, for example, the intense and spatially very confined electric fields that have been observed near the ionospheric projection of the plasmapause around 60° invariant latitude, often in relation to substorm activity [e.g., *Anderson et al.*, 1991]. The high resolution of the Freja measurements,

in particular using the burst memory, allows these intense electric field structures to be examined in detail.

In addition, the on-board memory can be and has been used to collect low-resolution data from many consecutive full orbits. This enables the study also of equatorial phenomena. One example of such a phenomenon are the so-called plasma bubbles that have been observed at lower altitudes by, for example, the San Marco D satellite [e.g., *Aggson et al.*, 1992]. Whether these structures can extend or propagate to higher altitudes has so far been an open question. Another example are Pc-1 pulsations where the satellite data can complement low-latitude ground magnetometer observations.

3. Experiment description

3.1 Measured quantities

The basic quantity measured by the electric field experiment, F1, is the electric field, which is determined from the potential difference between opposing probes. Since the probes are all in the spin plane of the satellite, only two components of the electric field are directly measured. The third component, along the spin axis, is not measured directly, but can be deduced from the other two using certain assumptions. (As a complement to the double-probe measurements the electric field is also measured by an electron-beam experiment, F6.) Normally, four of the spherical probes are used for electric field measurements, which produces a vector measurement with full time resolution. At times, however, only two probes are available for measuring E, in which case the electric field vector is available only when the electric field is sufficiently steady, and then with a time resolution corresponding to the spin period (6 s). The characteristics of the electric field measurement are found in Table 1.

Maximum field	1 V/m
Minimum field (bit resolution)	0.03 mV/m
Expected accuracy	$\approx$ 0.5 mV/m
Sampling rate, normal mode	768 s^{-1}
Sampling rate, burst mode	6144 s^{-1}

Table 1. Electric field measurement characteristics.

In addition to measuring the electric field, the F1 experiment also provides information on the satellite potential, giving a good indication of the relative plasma density variations of the ambient plasma.

The different quantities measured by the F1 experiment are the following:

- V_{12}, V_{34}, V_{56}: Potential differences between opposing probes
- V_1, V_2, V_3, V_4, V_5, V_6: Individual probe potentials with respect to the satellite
- V_{fg}: Floating ground potential, $\approx -$(Satellite potential)

- *HK*: Housekeeping data (temperatures, supply voltages, guard voltage, bias current, and amplitude detector output)

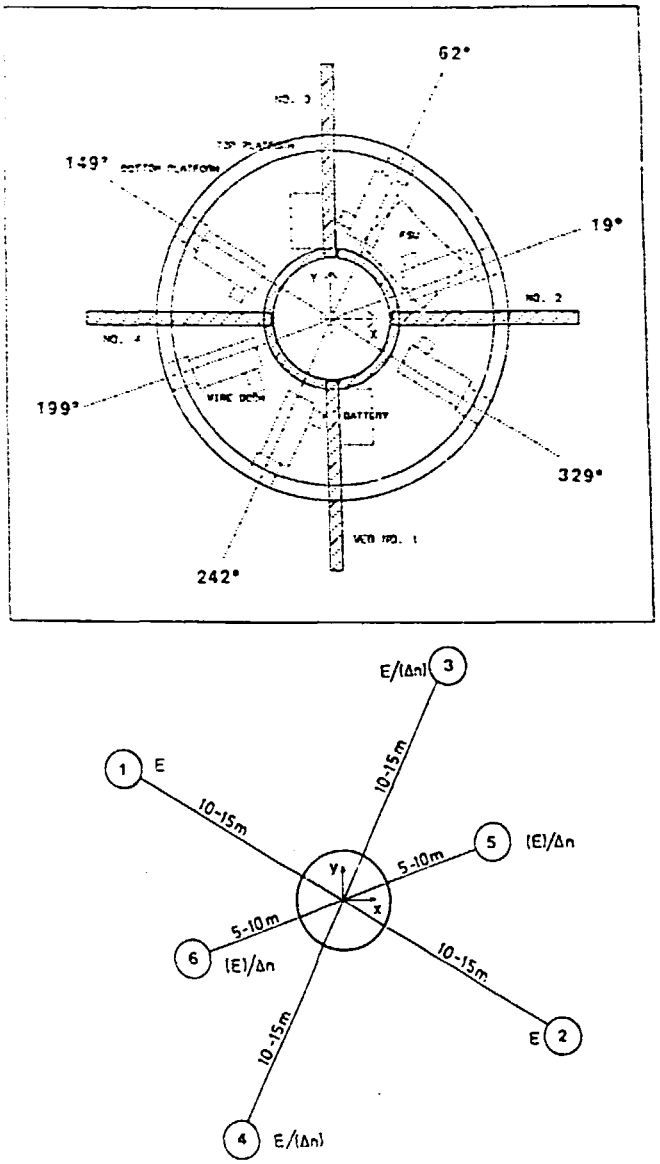

Fig. 1. F1/F4 wire boom and probe configuration.

3.2 Mechanical design

The electric field is measured with the double probe technique. Six spherical probes are used, extended on three wire boom pairs in the spin plane, as shown in Figure 1.

The probes are numbered from 1 to 6, and have a diametre of 6 cm. Probes 1 and 2 are used only for electric field measurements, and are extended to a distance of 10 m from the satellite (20 m tip–tip). Probes 3–6 may be used also by the F4 wave experiment for measurements of density fluctuations. Probes 3 and 4 are extended to 20 m tip–tip, whereas probes 5 and 6 are kept at a smaller distance (10 m tip–tip).

Figure 2 shows a more detailed picture of the geometry of the boom near the probe. On each side of the probe is a stub of length 8 cm, which was used to hold the probe during launch. On the inside of the inner stub is a section called the inner tip, with a length of 50 cm, and with the same diametre as the rest of the wire. The stubs and the tip are boot-strapped to the same potential as the probe. On the inside of the inner tip is a 10 cm long section of the wire, called the guard, which may be set to a negative potential to shield off the satellite potential from the probe. The wire boom itself is kept at satellite potential. Table 2 summarizes the dimensions and positions of the six wires and probes.

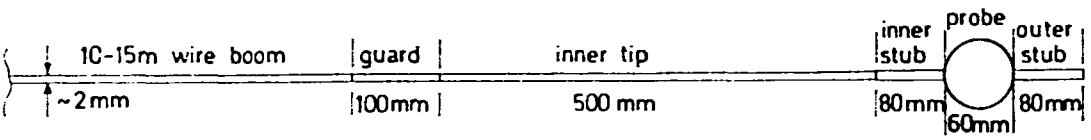

Fig. 2. Detailed view of the F1/F4 probe and boom geometry.

Probe number	1	2	3	4	5	6
Measured quantity	E	E	E or $\Delta n/n$	E or $\Delta n/n$	E or $\Delta n/n$	E or $\Delta n/n$
Angle from Freja x-axis	149°	329°	62°	242°	19°	199°
Probe diametre (cm)	6	6	6	6	6	6
Stub length (cm)	8	8	8	8	8	8
Inner tip length (cm)	50	50	50	50	50	50
Guard length (cm)	10	10	10	10	10	10
Boom length (m)	10(15)*	10(15)*	10(15)*	10(15)*	5(10)*	5(10)*
Boom diametre (mm)	2	2	2	2	2	2

* Current length (maximum possible length)

Table 2. Geometry and dimensions of the probe-boom-system.

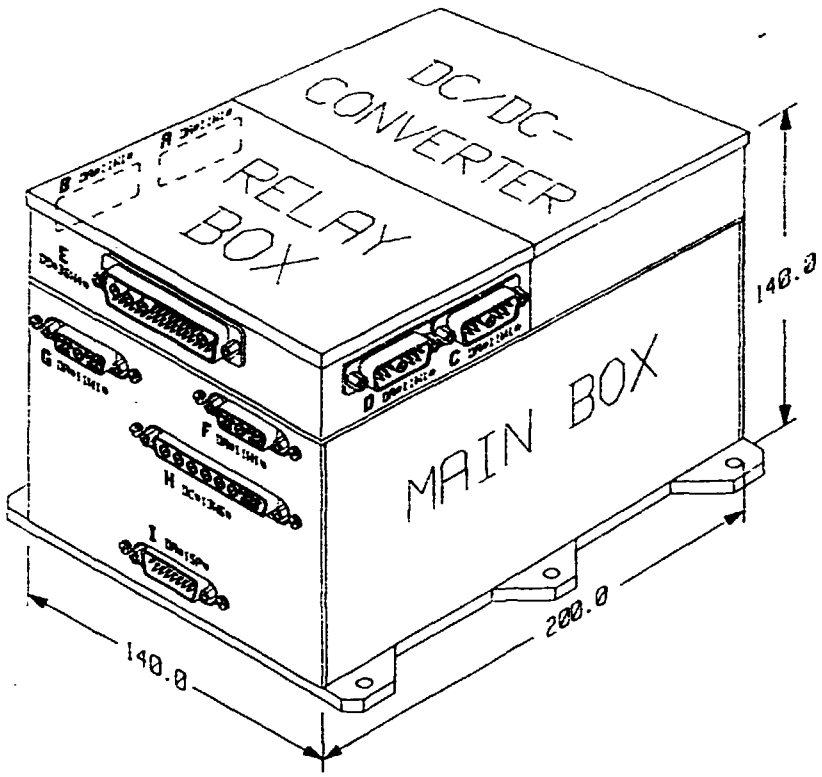

Fig. 3. The F1 electronics box.

Figure 3 shows the geometry of the F1 electronics box on top of which the DC/DC converter and relay box (for timesharing with F4) are attached. The dimensions of the electronics box, including DC/DC-converter and relay box, are 200 mm x 140 mm x 140 mm. The mass of the F1 experiment is 4.871 kg (excluding the wire booms), as specified in Table 3.

Electronics box	3.874 kg
Probes	4 x 0.18 kg
Harness and connectors	0.277 kg
Total	4.871 kg

Table 3. F1 mass budget.

3.3 Electrical design

A block diagram of the electric field experiment is shown in Figure 4. The signals from the six probes to the left are fed via preamplifiers, located in the probes,

through multiplexers and filters to the analog–to–digital converters (ADCs) seen in the right half of the Figure. The upper three ADCs are used to measure differential signals between the probes, and the lower two ADCs are used for measurement of the individual probe signals, as well as of the experiment housekeeping data and floating ground potential. The experiment is controlled by a microprocessor, which is reprogrammable by commands from the ground station. A 2 Mbyte burst memory is included to enable measurements with increased time resolution during selected time intervals, and for temporary storage of data.

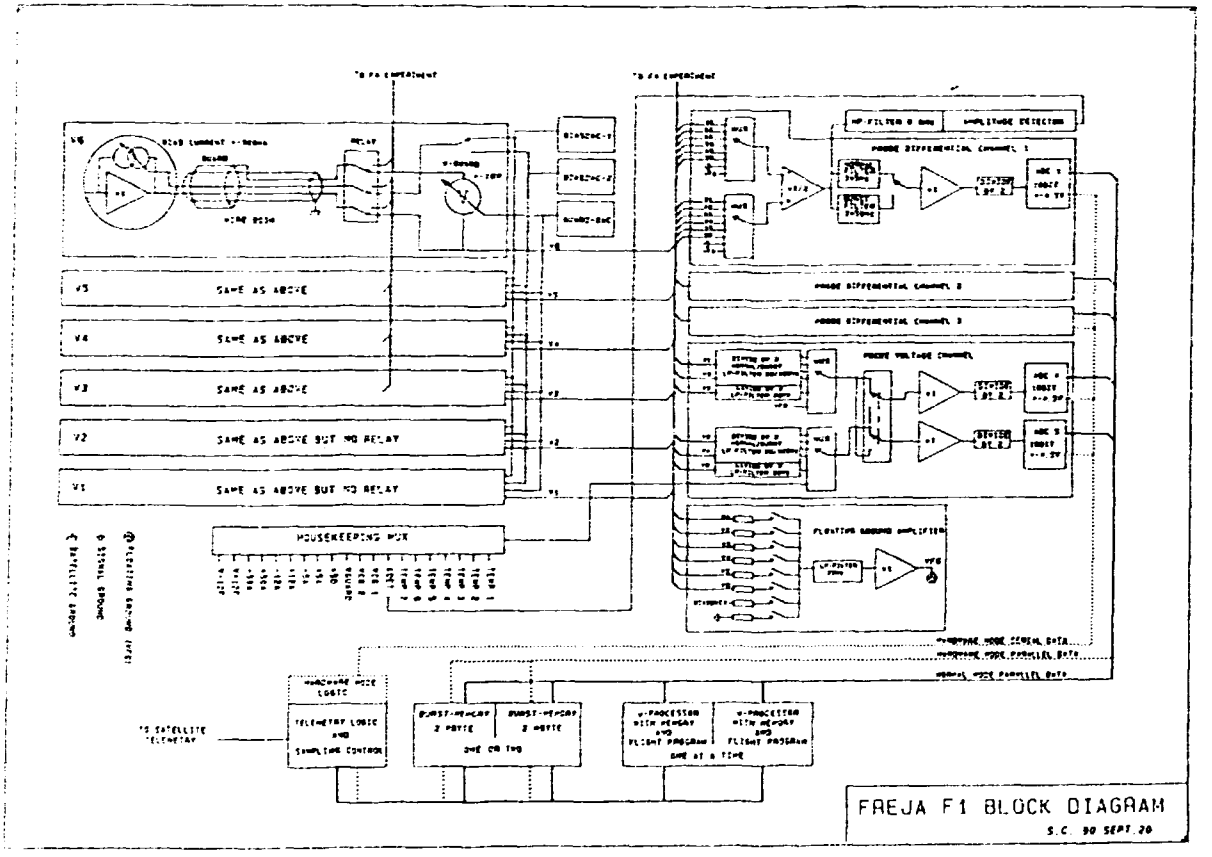

Fig. 4. Block diagram of the F1 electric field experiment.

The experiment contains a certain amount of redundancy to cover possible hardware failures. The signals from the probes may be fed to the ADCs along several different paths, to compensate for failures in the multiplexers or the ADCs. There is also a backup microprocessor identical to the primary one. The burst memory consists of two fully interchangeable memories of 2 Mbytes each, and these may also be run together to provide 4 Mbytes of storage. The 4 Mbyte configuration has actually been the normal mode of operation during the first six months of the mission. In the unlikely event of a complete processor failure, it is also possible

to run the experiment in a hardware mode, with reduced flexibility (note that the burst memory may still be used).

Four of the probes (number 3–6) are switchable with relays between the F1 and F4 experiments. F4 controls the probes completely when operating them in the $\Delta n/n$ mode. The signals from the probes operating in the electric field mode are sent also to the F4 experiment, for high-frequency wave analysis.

To optimize the quality of the measurement, the probes need to be kept close to the plasma potential. This is done by applying a bias current to the probe, which in sunlight compensates for photo-electron loss (negative bias current), and in shadow compensates for excess electron current from the ambient plasma (positive bias current). The current is controlled by the bias current digital–to–analog converter (BIASDAC) and may be set in the range ±900 nA. Two different values of the bias current may be applied simultaneously to different sets of probes (e.g., the probes on the long booms may have a different bias current from those on the shorter booms). For the specific plasma conditions experienced by the Freja satellite the bias current which has been found optimal for high-quality measurements is a small, positive value, typically 20 nA.

To minimize disturbances from the satellite and from the inner part of the boom, a 10 cm segment of the wire boom, called the guard, may be set to a certain potential with respect to its corresponding probe. This guard potential is controlled by the guard digital–to–analog converter (GUARD-DAC), and may be set in the range ±10 V. The guard voltage has normally been kept zero during the first six months of operations. In order to extend the voltage range of the measurements, a floating ground reference is used within the experiment. This floating ground voltage, V_{fg}, is set to be the average of the potential of selected probes. (It may also be set to a fixed value, for test purposes, using BIASDAC–2.) Normally it is set to the average of the potential of probes 1 and 2. This quantity is also of scientific value. Since the probes are actively kept near the plasma potential, V_{fg} is approximately equal to the negative of the satellite potential, which in turn depends primarily on the ambient electron density and, to a lesser degree, on the electron temperature. Thus, V_{fg} is a good indicator of plasma density variations.

Electronics	6.49 W
Probes	2 x 0.08 W (E probes)
	4 x 0.14 W (E/δn probes)
Subtotal	7.21 W
DC/DC losses	2.16 W (efficiency 77 %)
Total	9.37 W

Table 4. F1 power budget.

The differential signal V_{12} from probes 1 and 2 is fed into a special detector, seen at the top right of Figure 4. This detector consists of a high pass filter, to

remove the spin frequency from the signal, followed by an amplitude detector, which responds to rapid variations in the input signal (time constant $\tau = 68$ ms), and keeps the peak value for a certain time period ($\tau = 6.8$ s). The output, fed into the housekeeping multiplexer, is sampled once every 2 s, and may be used by the processor to trigger burst data collection (see also Sec. 4.1.1).

The F1 electric field experiment uses a total power of 9.37 W, as specified in Table 4. The numbers represent the estimated power after 6 months of operation.

3.4 Telemetry and sampling rates

Of the total normal Freja telemetry rate of 262.144 kbits/s, 30.720 kbits/s is allocated to the electric field experiment. The normal sampling rate for the electric field measurements is then 768 s^{-1}, corresponding to a time resolution of 1.3 ms. The possibility to double the overall telemetry rate to 524.288 kbits/s, is used for selected orbits (typically 1–2 per day) in which case also the electric field sampling rate increases by a factor of two.

For certain selected intervals of specific interest a sampling rate of 6144 s^{-1} is used to resolve the fine scale spatial and temporal variations of the electric field. This is possible by using the burst memory. The burst memory is also used to collect data when the satellite is not seen from any ground receiving station, and for collecting overview data with a low sampling rate (8 s^{-1}) from entire orbits.

No of Probes	Signals	Samples/s				
		Burst mode	Normal mode		Compressed mode	Overview mode
			Lo TM-rate	Hi TM-rate*		
2	V_{12}	6144	1536	3072	384	16
	V_1, V_2	768	128	256	32	1.33
	V_{fg}	32	32	64	8	0.33
3-4	V_{12}, V_{34}	6144	768	1536	192	8
	V_1, V_2, V_3, V_4	768	64	128	16	0.67
	V_{fg}	32	32	64	8	0.33
5-6	V_{12}, V_{34}, V_{56}	—	384	768	96	4
	$V_1, V_2, V_3, V_4, V_5, V_6$	—	64	128	16	0.67
	V_{fg}	—	32	64	8	0.33

* If any data other than "Normal mode" data are being stored in the memory, the column "Lo TM-rate" is applicable

Table 5. F1 sampling rates.

Due to the various operational conditions with different number of available probes, different sampling rates and telemetry rates a large number of operating modes are possible. For a more detailed description of these modes see Sec. 4. The sampling rates of the various signals for different operating modes are seen

in Table 5 (Lo TM-rate = 262.144 kbits/s, Hi TM-rate = 524.288 kbits/s). In addition, Table 6 shows the sampling rates in the hardware mode, which will be used in the unlikely event of a complete processor failure.

The F1 telemetry is described in more detail by *Bylander* [1993] and *Lindqvist et al.* [1993].

No of probes	Mode	Signals	Samples/s	
			Lo TM-rate	Hi TM-rate
2-6	Normal mode, real-time data	V_{12}, V_{34}, V_{56} V_1, V_2, V_3, V_4, V_{fg}	384 96	768 192
2-6	Normal mode, stored data	V_{12}, V_{34} V_1, V_2, V_3, V_4	768 96	768 96
2	Burst mode	V_{12} V_1, V_2	6144 768	6144 768
3-6	Burst mode	V_{12}, V_{34} V_1, V_2, V_3, V_4	6144 768	6144 768

Table 6. F1 sampling rates, hardware mode.

4. Modes of operation

The basic operating mode of the F1 experiment is the normal mode, which is used during real time data taking. In addition, four modes of operation are available when storing data in the burst memory for later transmission to ground: burst, normal, compressed and overview. The sampling rates in each mode are dependent on the number of probes used by the instrument. The telemetry format for the various modes and for the different number of probes is given in the separate document referred to above, and summarized in Tables 5 and 6. It is possible to store a succession of different modes in the memory, e.g., burst data surrounded in time by normal data.

Table 7 summarizes for the various modes the data collection intervals (ΔT) and distances travelled (ΔL) corresponding to a memory size of 2 MByte, the time and spatial resolutions of the measurements (Δt and Δl) and finally targets of suitable scales to be investigated (cf. Figure 5).

Mode	ΔT	ΔL	Δt(ms)	Δl(m)	Targets
Burst	67 s	470 km	0.16	1	Discrete arc
Normal	9.1 min	3800 km	1.30	10	Auroral oval
Compressed	36.4 min	15000 km	5.20	40	Few oval crossings
Overview	14.6 hrs	58 R_E	125	1000	Many orbits

Table 7. Coverage and resolution in different modes.

4.1 Burst mode

The burst mode (Figure 5a) allows about 1 minute of high-resolution data taking (0.16 ms) and is ideally suited for, e.g., studies of the fine structure of auroral arcs or auroral rays. The available distance of 470 km allows a good coverage of several arc structures and also of the ambient plasma in which the arcs are embedded.

4.1.1 Burst mode triggering

The burst mode may be triggered by

- An internal algorithm, based on the output from the amplitude detector described in Sec. 3.3. This trigger is also available to the Freja System Unit (FSU) for triggering a common burst mode in all the experiments.
- A command, which in turn may be sent
  - directly from the ground in real time
  - as a stored command at a pre-determined time
  - by the Freja System Unit upon receipt of a trigger signal in the on-board TM from one of the on-board experiments

During a common burst data taking period, when all the Freja experiments are run in their burst mode, it has been agreed that a time period of at least 30 s following the burst trigger is common to all experiments. In addition, each experiment may choose to store data before the trigger, or for a longer time than 30 s after the trigger. During the first 6 months of operations, common bursts have been triggered both by time-tagged commands and by event detectors in several of the experiments. For example, the burst data collection on orbit 1694 was triggered by the F1 amplitude detector. These data are further discussed in the section on scientific results. In the electric field experiment, the amount of data saved in the memory before the trigger can be set to 0, 14, 28, 43, 57, 72, 86, or 100 %. For example, if 14 % is chosen, this means that 9.5 s data are stored before the trigger, and 57.5 s after the trigger. It is possible to store several segments of data in the memory, but only if no pre-trigger data (0 %) are stored. The different segments need not be collected in the same mode, and it is thus possible to store a segment of burst mode data surrounded by normal mode data.

4.2 Normal mode

The normal mode is used for real time data taking, but may also be used when storing data in memory. The full memory size in this case corresponds to about 9

minutes of data and a distance ΔL of 3800 km to be covered with a time resolution of approximately 1 ms (Figure 5b). This mode is ideally suited for detailed studies of large-scale auroral phenomena that involve a significant part of the auroral oval and adjacent regions. In this mode the rate of data collection to the memory is the same as the normal TM bit rate of 30.72 kbits/s allocated to the F1 experiment.

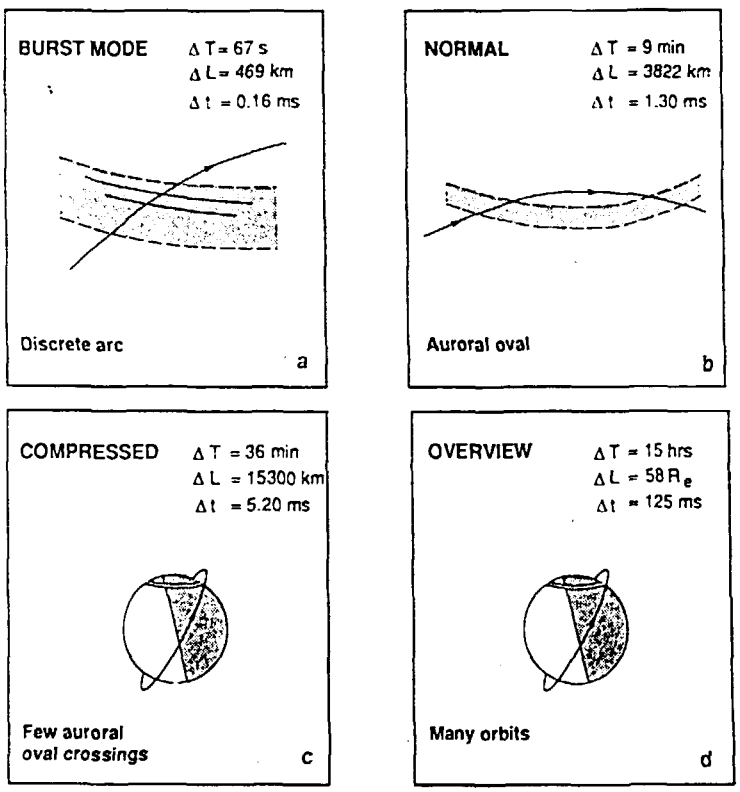

Fig. 5. F1 modes of operation.

4.3 Compressed mode

In the compressed mode (Figure 5c) the sampling rate is decreased by a factor of 4 as compared to the normal mode. This allows 36 minutes of data with a time resolution of about 5 ms to be stored, and is occasionally used to store several auroral crossings or other interesting areas during a period when the satellite is not seen from a ground station.

4.4 Overview mode

In the overview mode (Figure 5d) the sampling rate is even further decreased to 8 samples/s. This allows storage of several complete orbits in the memory, which is useful for statistical studies of the global electric field behaviour. This mode is normally used in conjunction with a corresponding mode of the magnetic field experiment, F2.

4.5 Memory dumping

Freja is typically in contact with Esrange about 2 hours/day distributed over about half of the total 13 orbits/day. With the given TM-rate of 262 kbits/s or 524 kbits/s it takes about 10 or 5 minutes, respectively, to empty the memory. It is therefore possible to dump the full memory contents during a majority of the orbits that are within contact from Esrange. In between this set of orbits there are typically as many as 5–6 orbits or 10–12 hours with no Esrange contact. The other ground station at Prince Albert, Canada, has similar contact conditions to those of Esrange.

It is not possible to dump the memory contents to TM while new data are being stored in the memory. It is not necessary to dump the entire memory at once, but it may be spread out over several time periods. It is possible to use the memory for storing data also in the hardware mode, but with some reduction in flexibility. For example, the compressed mode and the overview mode are not available, and the triggering can only be done by ground command with no pre-trigger data stored.

4.6 Langmuir mode

In addition to the above mentioned modes for measuring the electric field, there is a mode called the Langmuir mode. In this mode, the bias current to the probe is swept between –900 nA and +900 nA, and the potential of the probe is measured. This current sweep is used primarily to help in setting the appropriate bias current for electric field measurement, but may also be used to determine plasma density and temperature. An automatic algorithm may be run on-board to determine the optimum operating bias current. Normally, however, the bias current is set by ground command. The time interval between current sweeps and their duration are set by ground command, and are typically of the order of 30 s and 300 ms, respectively.

5. Preliminary scientific results

5.1 Freja scientific operations

A system for coordinating the Freja scientific operations was developed by the F1 team. The system, which has been accepted and adopted by all Freja PI-groups, includes strategies for the data taking and data dumping and guidelines for the day-to-day practical handling and interface with Freja Operations Centre. In particular, the extensive information available in the Freja orbit characteristics plots, produced and distributed by the F1 team, are used as a guide for the selection of science and other modes for coordinated and non-coordinated operations, respectively.

Figure 6 shows a slightly modified version of a Freja orbit characteristics plot for November 12, 1992, including in addition to the orbit and geophysical parameters also F1 electric field observations. The panels show from top to bottom the Freja altitude, the invariant latitude of Freja and the latitude of the equatorward edge of the northern and southern standard oval, the magnetic local time of Freja, the maximum absolute value of the differential potential V_{12}, the mean of the measured probe potentials V_1 and V_2 (which closely follows the satellite potential but with opposite sign), the time segments for which Freja's footpoint is within the auroral

oval or polar cap and the angle between the magnetic field and the spin axis (pointing roughly towards the sun), the time segments for which Freja can be seen from Esrange, Prince Albert and Syowa and when Freja is in eclipse.

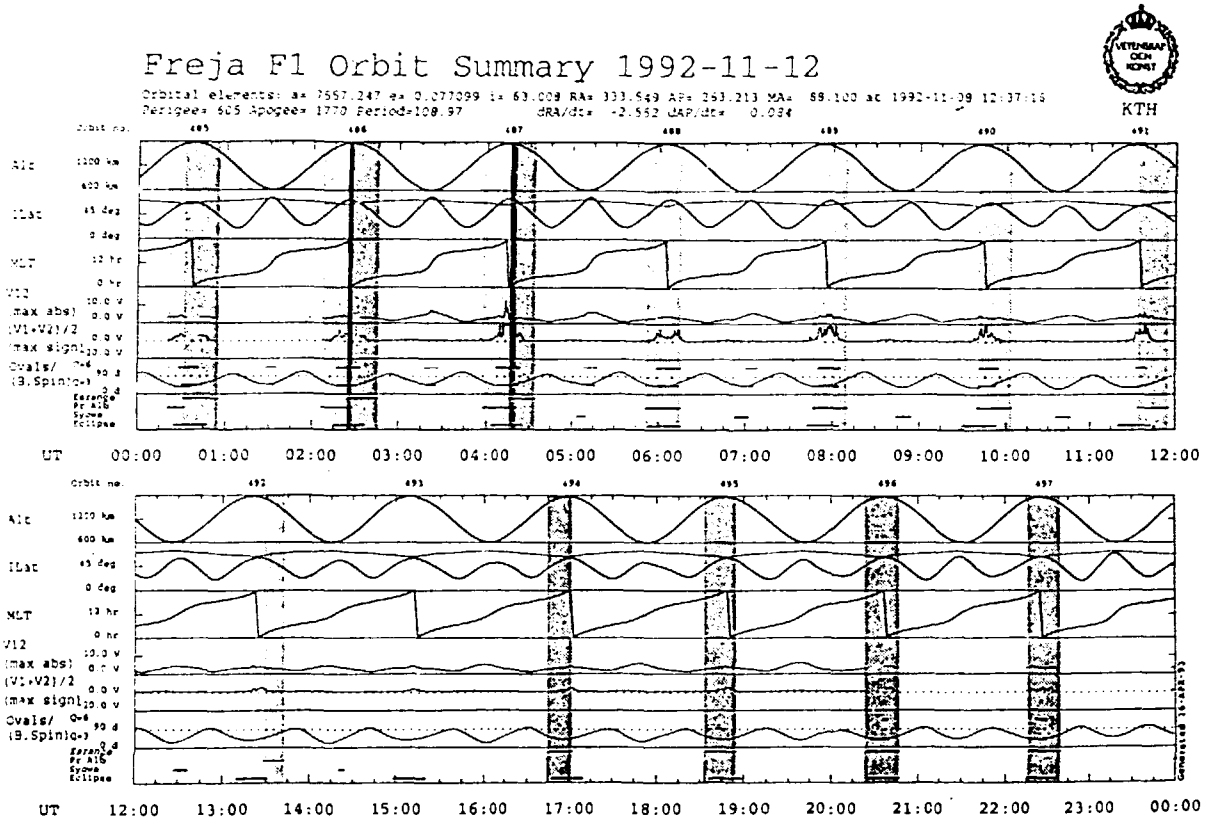

Fig. 6. Summary of Freja orbit characteristics and F1 electric field observations.

This plot is identical to the orbit characteristics plots produced by the F1 team with the only exception that F1 observations have replaced range and elevation in panels 4 and 5 to enable comparisons with the model predictions. Note that the locations of the intense variations seen in V_{12} and $(V_1+V_2)/2$, indicative of auroral activity, agree very well with the predicted encounters with the auroral and polar cap plasma. The example shown here illustrates that realistic predictions are provided by the orbit characteristics plots and that they constitute a most valuable tool for the scientific planning and selection of interesting orbits (and scientifically less interesting orbits which can be used for memory dumping).

5.2 The fine structure of intense, irregular electric fields

Figure 7 shows high resolution electric field data (6144 samples/s) of very intense electric fields observed on Freja orbit 1694 during a Prince Albert pass on February 11, 1993. The observations were made in the postmidnight sector near 0100 MLT and 66° corrected geomagnetic latitude. The coordinate system used for

the presentation of the data is a satellite-oriented system defined by the projection of the model magnetic field (IGRF90) into the satellite spin plane (axis 1), the direction of the satellite spin axis (axis 3, pointing roughly towards the sun), and axis 2 in the spin plane (perpendicular to the magnetic field and pointing roughly towards dusk), which completes the orthogonal right-hand system. The top and the middle panels show the two measured spin plane components, E_{1msp} and E_{2msp}, and the bottom panel the spin axis component, E_{3msp}, which has been estimated using the assumption that the magnetic-field-aligned electric field component is zero.

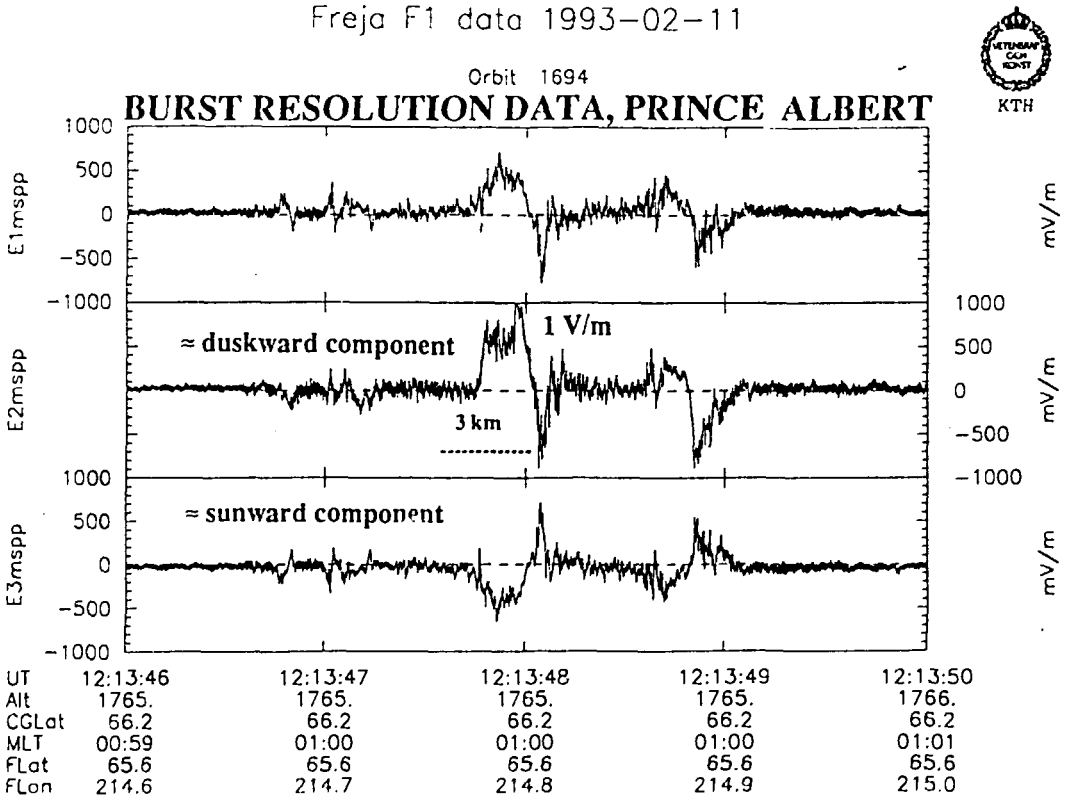

Fig. 7. Burst resolution data showing the fine structure of intense electric fields.

In this event two nearby intense structures are seen having magnitudes of about 1 V/m and characteristic widths of 3 km, corresponding to 2 km at ionospheric altitude. For both of the structures the electric field is found to be pointing away from the centre (positive divergence), opposite to what is normally the case for the electric fields associated with auroral arcs. The structures occur at the edge of a large-scale downward field-aligned current sheet adjacent to a large-scale upward field-aligned current sheet. In addition a very complicated system of fine-scale multiple up- and downward field-aligned current sheets or filaments related to the

structures can be inferred from the magnetometer data (*L. J. Zanetti, private communication*). The particle data show perpendicular ion fluxes but an absence of precipitating electrons. The structures are further associated with significant wave activity with broad band electrostatic noise up to kHz frequencies, the upper limit being set by the burst sampling rate of the instrument.

A 2 km scale size was also found to be characteristic for individual electric field structures observed on auroral field lines at high altitude by the Viking satellite [cf. *Marklund*, 1993]. Such arc-associated electric field structures and ULF pulsations both contribute to the low-frequency electric field fluctuations peaking around 0.5–1 Hz as observed in the Viking electric field data. A clear correlation was found between the intense low-frequency electric field fluctuations and the transversely energized ions as observed at lower altitudes by Viking [cf. *Lundin et al.*, 1990]. The Freja data suggest that such a correlation exists also at Freja altitudes.

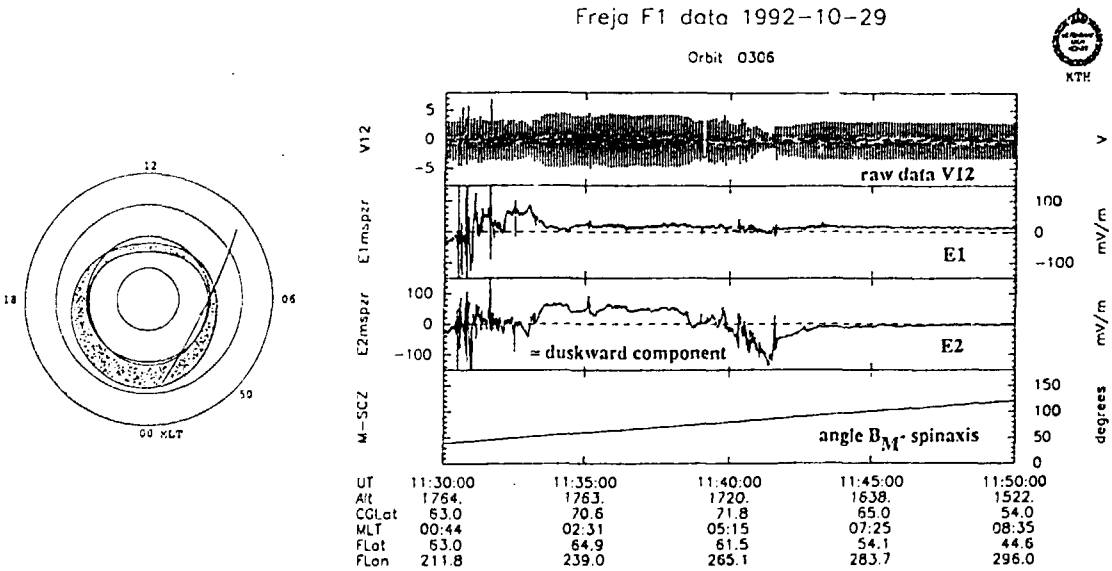

Fig. 8. Normal resolution electric field data from an auroral oval crossing.

5.3 Electric field observations from oblique auroral oval crossings

Figure 8 shows normal resolution electric field data (768 samples/s) from an auroral oval crossing of the kind illustrated in Figure 5b. The data are from a Prince Albert pass, orbit 306, on October 29, 1992. The upper panel shows the raw data signal, V_{12}, in the frame of reference of the spinning spacecraft, thus including the $\mathbf{v} \times \mathbf{B}$ induced electric field. The electric components shown in the second and third panel are the two spin plane components E_{1msp} and E_{2msp} after despinning and subtraction of $\mathbf{v} \times \mathbf{B}$ from the raw data. The third panel shows the angle between the direction of the spin axis and the model magnetic field,

which is seen to vary considerably during the pass. Around 1140 UT when the angle is close to 90° (the magnetic field is in the spin plane) the E_{1msp} and E_{2msp} represent the parallel (to B) and the duskward (perpendicular to B) electric field components, respectively. At other times the perpendicular electric field enters into both components. In the beginning of the pass around 1130 UT Freja is above the midnight auroral oval, recognized by the intense electric field fluctuations (>100 mV/m) in both components. Between 1133 UT and 1138 UT Freja is in the polar cap and a relatively stable electric field of about 50 mV/m can be seen in the E_{2msp} component. An electric field reversal from a duskward (poleward) field in the polar cap to a dawnward (equatorward) field in the morningside oval occurs around 1140 UT. Note the extreme extension of this reversal region (1200 km) which can be observed due to the fact that Freja covers a wide local time sector during its traversal through the auroral oval. The Freja orbit offers excellent opportunities to explore phenomena associated with large east-west gradients such as the Harang discontinuity, the westward travelling surge and the region behind the surge which often contains north-south oriented auroral arc structures.

OVERVIEW OF AN OBLIQUE AURORAL OVAL CROSSING

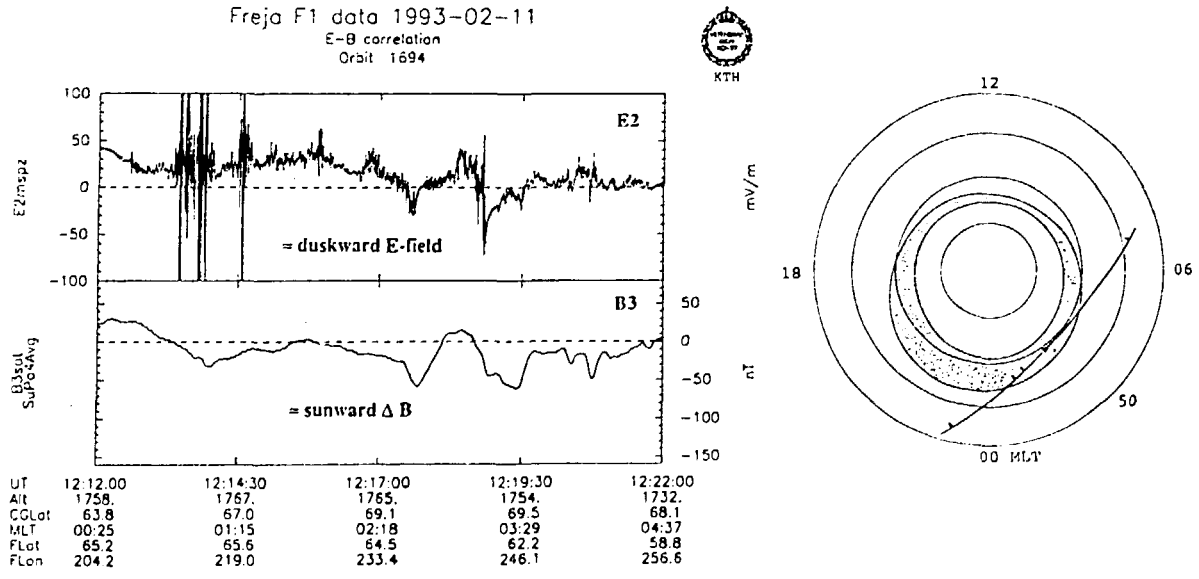

Fig. 9. Electric and magnetic field data from an oblique auroral oval crossing.

Figure 9 shows electric and magnetic field data from another oblique auroral oval crossing during orbit 1694, which was discussed in the previous section. The intense electric field structures are recognized as the second group of electric field spikes (from the left) that exceeds 100 mV/m around 1213:50 UT. Throughout the oval crossing the large-scale variations in the duskward electric field component are seen to be nicely correlated with the sunward magnetic field component.

Such a correlation results from field variations due to the satellite motion over spatial structures coupled by field-aligned currents to ionospheric regions of relatively homogeneous conductivity [cf. *Sugiura et al.*, 1982]. For this case the ratio of magnetic to electric field variation gives a value of the height-integrated Pedersen conductivity of 0.7 S. These large-scale field-aligned current sheets are presumably associated with auroral arc structures being oriented nearly in a north-south direction.

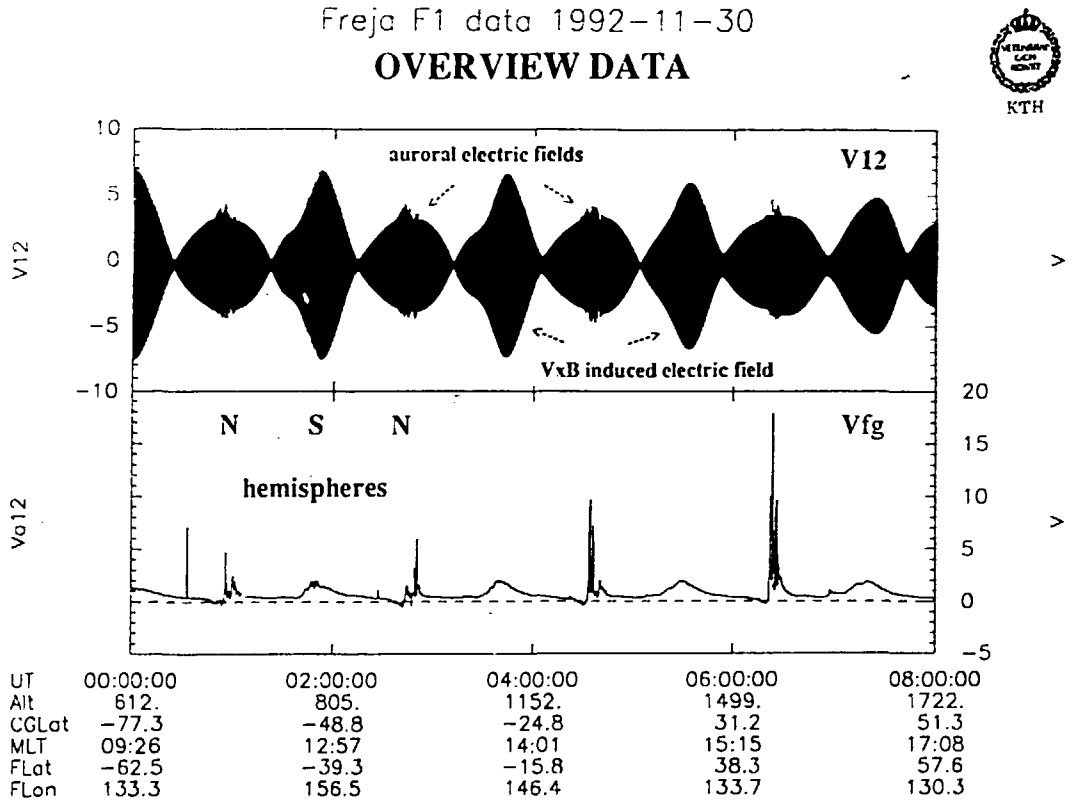

Fig. 10. Overview electric field data from four consecutive Freja orbits.

5.4 Subauroral, mid- and low-latitude electric fields

One of the great advantages with the Freja electric field instrument is its capability to store data from entire orbits. An example of overview raw data collected from 4 consecutive orbits is shown in Figure 10. The top panel shows the raw differential signal V_{12} (8 samples/s) and the bottom panel the floating ground potential (roughly the negative of the satellite potential). The "sausages" are formed by the envelope of the $\mathbf{v} \times \mathbf{B}$ induced electric field which twice per orbit becomes very small (or zero) as Freja passes the magnetic equator (where the satellite velocity vector is nearly parallel to the magnetic field). The smaller "sausages" correspond to high-altitude northern hemisphere crossings ($\mathbf{v}$ smaller and $\mathbf{B}$ weaker). At high

latitudes the auroral electric fields are recognized by the irregular fluctuations superposed on the $\mathbf{v} \times \mathbf{B}$ induced electric field as well as by the intensifications of the floating ground potential. Note that these electric fields are much more intense for the northern hemisphere crossings which mainly has to do with the prevailing orbit geometry with apogee above the nightside auroral oval (and polar cap region) in the northern hemisphere and perigee above the dayside subauroral region in the southern hemisphere. In addition the higher altitude and the prevailing winter conditions in the northern hemisphere both contribute to the more structured and intense electric fields observed there. The overview data thus enable a complete coverage of all northern and southern auroral oval encounters by the Freja satellite. A number of interesting results from subauroral and low-latitude regions have been revealed from the overview data, such as the frequent occurence of intense electric fields near the ionospheric projection of the plasmapause (presumably related to the plasmatrough).

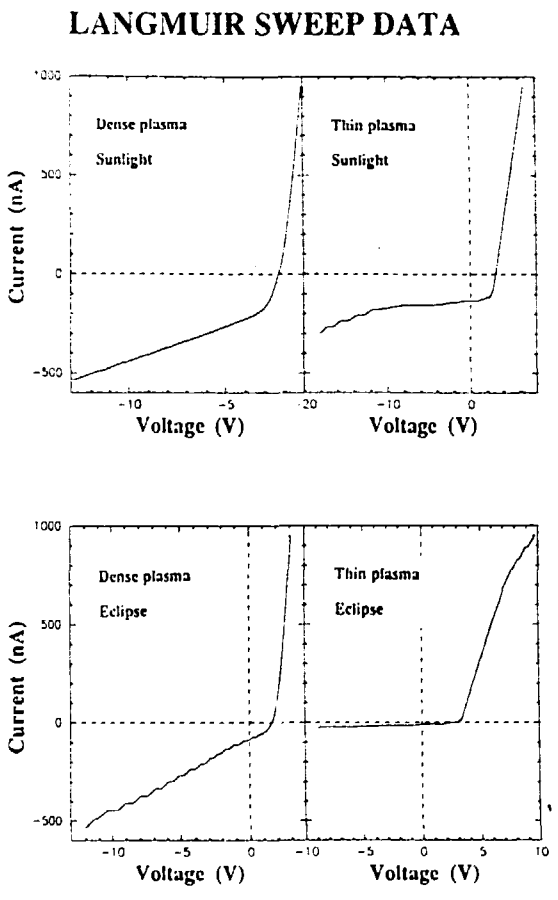

Fig. 11. Current-voltage characteristics in different plasma environments.

5.5 Monitoring of the Freja plasma environment

Examples of current-voltage characteristics representative of the different plasma environments encountered by the Freja satellite are shown in Figure 11. The plots show the bias current versus the potential measured between the biased probe and

the opposing probe at floating potential ($I = 0$). From analysis of these $I - V$ characteristics the plasma density and temperature are derived.

The examples shown are from (a) a dense sunlit plasma, (b) a thin sunlit plasma, (c) a dense plasma in eclipse, (d) a thin plasma in eclipse. The photoelectron current is given by the difference between the zero level and the knee of the $I - V$ curve, which for the examples shown here amounts to about 100 nA. Note the difference in the slopes of the $I - V$ curves in the ion saturation regime for the dense and thin plasma. The intermittent current sweeps (max repetition frequency, 2 s^{-1}) combined with the floating ground potential measurement (32 samples/s) provide a very valuable monitoring of the different plasma environments explored by Freja.

6. Summary

A sophisticated double-probe electric field instrument for high-resolution measurements of the auroral fine structure has been developed for the Freja mission. The instrument is equipped with a 4 Mbyte burst memory for high-rate data sampling (6144 samples/s) and for temporary storage of data. It can be run in a number of different operational modes and provides information not only on the vector electric field but also on the satellite potential (i.e., roughly the plasma density) with a time resolution orders of magnitude better than on previous satellite missions.

The plasma environment explored by Freja, i.e., the plasma transition region between the upper ionosphere and the innermost magnetosphere, is a highly dynamic region characterized by a considerable degree of spatial and temporal structure on various scales, and is associated with various phenomena such as intense, irregular electric fields, weak double layers, transient electric fields, and low-frequency electric field fluctuations. The preliminary results from the first six months of operation clearly demonstrate that the Freja electric field instrument with its burst memory capability and possibility of simultaneous vector electric field and interferometric density measurements is ideally suited for detailed studies of these phenomena. Moreover, the measurements may contribute significantly to our understanding of different aspects of the auroral electrodynamics such as the formation, energy transfer, and current closure mechanisms of different auroral arc structures (westward travelling surges, multiple arcs, Ω bands, etc.) and, more generally, of the relationships between auroral electric fields, currents, particles, and optical emissions.

Acknowledgments. The authors are grateful to the large number of people who have contributed to the success of the project. In particular we want to acknowledge the eminent work in instrument and software development performed by the hardware and software engineering teams at the Royal Institute of Technology, namely, Lars Bylander, Ola Carlström, Sverker Christenson, Göran Olsson, Bengt Harald Nilsson, and Ramesh Mehra. Valuable contributions in the hardware development have also been made by the engineering team of the Department of Physics, Oulu University. The Freja project was supported by the Swedish National Space Board and by the German Ministry for Research and Technology (BMFT). The

Freja satellite is managed and operated by the Swedish Space Corporation under contract from the Swedish National Space Board.

References

Aggson, T. L., N. C. Maynard, W. B. Hanson, and J. L. Saba, Electric field observations of equatorial bubbles, *J. Geophys. Res., 97*, 2997, 1992.

Anderson, P. C., W. B. Hanson, and R. A. Heelis, The ionospheric signatures of rapid sub-auroral ion drifts, *J. Geophys. Res., 96*, 5785, 1991.

André, M. and L. Eliasson, Electron acceleration by low-frequency electric field fluctuations: Electron conics, *Geophys. Res. Lett., 19*, 1073, 1992.

Blomberg, L. G. and G. T. Marklund, High-latitude electrodynamics and aurorae during northward IMF, in *Dynamics of Auroral Plasma, AGU Monograph, in press*, 1993.

Boström R., G. Gustafsson, B. Holback, G. Holmgren, H. Koskinen, and P. Kintner, Characteristics of solitary waves and weak double layers in the magnetospheric plasma, *Phys. Rev. Lett., 61*, 82, 1988.

Bylander, L., The double probe electric field experiment on Freja: User's guide and reference manual, *Royal Inst. of Technol. Report ALP-1993-105*, 1993.

Hultqvist, B., On the acceleration of electrons and positive ions in the same direction along magnetic field lines by parallel electric fields, *J. Geophys. Res., 93*, 9777, 1988.

Hultqvist, B., H. Vo, R. Lundin, B. Aparicio, P.-A. Lindqvist, G. Gustafsson, and B. Holback, On the upward acceleration of electrons and ions by low-frequency electric field fluctuations observed by Viking, *J. Geophys. Res., 96*, 11609, 1991.

Lindqvist, P.-A. and G. T. Marklund, A statistical study of high-altitude electric fields measured on the Viking satellite, *J. Geophys. Res., 95*, 5867, 1990.

Lindqvist, P.-A., L. G. Blomberg, B. H. Nilsson, L. Bylander, and G. T. Marklund, The double probe electric field experiment on Freja: Telemetry format description, *Royal Inst. of Technol. Report ALP-1993-103*, 1993.

Lundin, R., G. Gustafsson, A. I. Eriksson, and G. T. Marklund, On the importance of high-altitude low-frequency electric field fluctuations for the escape of ionospheric ions, *J. Geophys. Res., 95*, 5905, 1990.

Mälkki, A., A. I. Eriksson, P.-O. Dovner, R. Boström, B. Holback, G. Holmgren, and H. E. J. Koskinen, A statistical survey of auroral solitary waves and weak double layers: 1. Occurence and net voltage, submitted to *J. Geophys. Res.*, 1993.

Marklund, G. T., Viking investigations of auroral electrodynamical processes, *J. Geophys. Res., 98*, 1691, 1993.

Marklund, G. T. and L. G. Blomberg, Toward a better understanding of the global auroral electrodynamics through numerical modeling studies, in *Magnetospheric Substorms, AGU Monograph 64*, 305, 1991.

Sugiura, M., N. C. Maynard, W. H. Farthing, J. P. Heppner, and B. G. Ledley, Initial results on the correlation between the magnetic and electric fields observed from the DE–2 satellite in the field-aligned current regions, *Geophys. Res. Lett., 9*, 985, 1982.

Temerin M., K. Cerny, W. Lotko, and F. S. Moser, Observations of double layers and solitary waves in auroral plasma, *Phys. Rev. Lett., 48*, 1175, 1982.

Weimer D. R., C. K. Goertz, D. A. Gurnett, N. C. Maynard, and J. L. Burch, Auroral zone electric fields from DE 1 and 2 at magnetic conjunctions, *J. Geophys. Res., 90*, 7479, 1985.

TRITA-ALP-1993-02
ISSN 1103-6613
ISRN KTH/ALP/R--93/2--SE

Royal Institute of Technology, Alfvén Laboratory,
Department of Plasma Physics, S-100 44, Stockholm, Sweden

THE DOUBLE PROBE ELECTRIC FIELD EXPERIMENT ON FREJA: DESCRIPTION AND FIRST RESULTS

G. T. Marklund, L. G. Blomberg, P.-A. Lindqvist, C.-G. Fälthammar, G. Haerendel, F. S. Mozer, A. Pedersen, and P. Tanskanen

October 1993, 23 pages, in English

A description is given of the Freja double-probe electric field instrument. Its capability to perform high-resolution measurements of the aurora and its fine-structure as well as collect information on sub-auroral and low-latitude phenomena is illustrated by selected results from the first six months of operation. The instrument is highly flexible and possible to operate in a number of different modes. It is also equipped with a 4-Megabyte burst memory for high data sampling rate and temporary storage of data. It has been fully operational since October 1992, and delivers data from ≈22 hours/day including about 5–6 auroral crossings/day of the northern and southern auroral ionosphere. New and important information on the auroral fine structure and electrodynamics is obtained by means of burst resolution data (6144 samples/s) and normal resolution data (768 samples/s). Common burst data collection triggered by the electric field event detector has turned out to be very useful for the selection of scientifically interesting events. This is illustrated by high-resolution data of a pair of extremely intense and narrow electric field structures (1 V/m) which are associated with a total absence of precipitating particles, depletions of the thermal plasma and with an intense wave activity. The low inclination of the Freja orbit provides a new perspective for studying large-scale phenomena associated with east-west gradients as is exemplified by electric field data from a satellite crossing over north-south oriented auroral structures presumably resulting from rotational distortions of east-west aligned auroral arcs. The different plasma regimes encountered by Freja are continuously monitored by means of current sweeps applied to the probes and by the satellite potential. In addition, overview data (8 samples/s) are collected from full orbits and stored in the on-board memory and have proved to be extremely valuable, providing new information on global electric field phenomena at subauroral and lower latitudes, such as the intense poleward electric fields and Pc–1 observations that have been made near the plasmapause during substorm activity.

Keywords: Aurora, Auroral particle acceleration, Electric fields, Equatorial phenomena, Freja electric field experiment, Freja satellite, Ionosphere, Magnetosphere, Sub-auroral phenomena